JOURNAL OF MOLECULAR SPECTROSCOPY **160**, 39–57 (1993)

The Potential Energy Surface for the Electronic Ground State of H_2Se Derived from Experiment

PER JENSEN*,[1] AND IGOR N. KOZIN†

** FB 9–Theoretische Chemie, Bergische Universität–Gesamthochschule Wuppertal, Gaussstrasse 20, W-5600 Wuppertal 1, Germany; and † Physikalisch-Chemisches Institut, Justus-Liebig-Universität Giessen, Heinrich-Buff-Ring 58, W-6300 Giessen, Germany*

The present paper reports a determination of the potential energy surface for the electronic ground state of the hydrogen selenide molecule through a direct least-squares fitting to experimental data using the MORBID (Morse oscillator rigid bender internal dynamics) approach developed by P. Jensen [*J. Mol. Spectrosc.* **128**, 478–501 (1988); *J. Chem. Soc. Faraday Trans. 2* **84**, 1315–1340 (1988)]. We have fitted a selection of 303 rotation–vibration energy spacings of $H_2{}^{80}Se$, $D_2{}^{80}Se$, and $HD^{80}Se$ involving $J \leq 5$ with a root-mean-square deviation of 0.0975 cm^{-1} for the rotational energy spacings and 0.268 cm^{-1} for the vibrational spacings. In the fitting, 14 parameters were varied. On the basis of the fitted potential surface we have studied the cluster effect in the vibrational ground state of H_2Se, i.e., the formation of nearly degenerate, four-member groups of rotational energy levels [see I. N. Kozin, S. Klee, P. Jensen, O. L. Polyansky, and I. M. Pavlichenkov, *J. Mol. Spectrosc.*, **158**, 409–422 (1993), and references therein]. The cluster formation becomes more pronounced with increasing J. For example, four-fold clusters formed in the vibrational ground state of $H_2{}^{80}Se$ at $J = 40$ are degenerate to within a few MHz. Our predictions of the $D_2{}^{80}Se$ energy spectrum show that for this molecule, the cluster formation is displaced towards higher J values than are found for $H_2{}^{80}Se$. In the vibrational ground state, the qualitative deviation from the usual rigid rotor picture starts at $J = 12$ for $H_2{}^{80}Se$ and at $J = 18$ for $D_2{}^{80}Se$, in full agreement with predictions from semiclassical theory. An interpretation of the cluster eigenstates is discussed.

I. INTRODUCTION

The present paper reports a determination of the potential energy surface for the electronic ground state of the hydrogen selenide molecule through a direct least-squares fitting to experimental data using the MORBID (Morse oscillator rigid bender internal dynamics) approach developed by Jensen (*1, 2*). The H_2Se molecule is a near-symmetric top in that two of its equilibrium rotational constants are almost equal. Further, its vibrational energy level spectrum shows marked local mode behavior (*3, 4*): some of the stretching energy levels form nearly degenerate pairs. The members of such a pair have a common value of $v_1 + v_3$, and the energy separation between them decreases with increasing $v_1 + v_3$. For H_2Se, this energy separation is about 0.1 cm^{-1} for $v_1 + v_3 = 3$.

However, the most unusual feature of the H_2Se rotation–vibration energy spectrum is the formation of nearly degenerate, four-member groups of energy levels. This cluster effect represents a significant deviation from the harmonic oscillator-rigid rotor picture employed in the customary treatment of molecular vibration and rotation. The cluster formation has been predicted for the vibrational ground state of H_2O by Zhilinskii

[1] Guest professor 1992–1993. On leave from Physikalisch-Chemisches Institut, Justus-Liebig-Universität Giessen, Heinrich-Buff-Ring 58, W-6300 Giessen, Germany.

0022-2852/93 $5.00

and Pavlichenkov (*5*) using semiclassical methods, and it has been discussed in detail by Makarewicz and Pyka (*6–8*) on the basis of semiclassical theory and model quantum mechanical calculations.

Very recently (*9–11*) the predicted four-fold clusters have been observed experimentally in the rotational spectrum of H_2Se and analyzed with a Watson-type Hamiltonian.

We aim at analyzing the unusual rotation–vibration energy spectrum of H_2Se through direct quantum mechanical calculations of the energy levels and wavefunctions on the basis of a potential energy surface for the electronic ground state. We carry out the calculations using the MORBID Hamiltonian and computer program (*1, 2*). The MORBID approach treats the complete rotational and vibrational motion of a triatomic molecule and calculates the eigenvalues of the rotation–vibration Hamiltonian variationally, that is, without the use of perturbation theory. MORBID allows the calculation of rotation–vibration energy levels directly from the potential energy surface with an accuracy comparable to that of other methods of this type (*12–14*), and it has the added advantage of being able to optimize the parameters of an analytical representation of the potential energy surface through a least-squares fitting to experimental data. Further, MORBID employs a clear physical picture in that the basis functions used for the variational calculation are tailored for the molecule in question. Hence it is generally possible to carry out a straightforward "spectroscopic" assignment of the calculated energy levels on the basis of the corresponding wavefunctions. This is particularly important when describing the highly excited rotational energy levels exhibiting the cluster effect.

As the starting point for our analysis we obviously require a potential energy surface for the electronic ground state of H_2Se. This surface has been calculated ab initio by Senekowitsch *et al.* (*15*). It is known, however (see, for example, the discussion by Fernley *et al.* (*16*)), that by optimizing the parameters of an analytical representation for the potential energy surface through least-squares fitting to experimental data, it is possible to obtain potential energy surfaces superior to those determined in ab initio calculations. For H_2Se, two surfaces have been obtained from experimental data: one by Halonen and Carrington (*4*) and one by Kauppi and Halonen (*17*). In both Ref. (*4*) and Ref. (*17*), the theoretical models used for H_2Se were also used for fitting potential energy surfaces of water, and Fernley *et al.* (*16*) have compared the resulting surfaces to one fitted by Jensen (*18*) using the MORBID approach. They found the MORBID surface to be more accurate than those from Refs. (*4*) and (*17*). In view of this, we have found it worthwhile to use the MORBID Hamiltonian for carrying out a least-squares fitting to experimental data for H_2Se and its isotopic species, thus obtaining a potential energy surface which can serve as a basis for our analysis of the cluster structure in the energy spectrum. The present paper reports this fitting.

We have fitted a selection of 303 rotation–vibration energy spacings of $H_2{}^{80}Se$, $D_2{}^{80}Se$, and $HD{}^{80}Se$ involving $J \leq 5$ with a root-mean-square (RMS) deviation of 0.0975 cm^{-1} for the rotational energy spacings and 0.268 cm^{-1} for the vibrational spacings. In the fitting, 14 parameters were varied. On the basis of the fitted potential surface we have predicted a large number of rotation–vibration energies. We find as expected that the cluster formation becomes more pronounced with increasing J. For example, four-fold clusters formed in the vibrational ground state of $H_2{}^{80}Se$ at J = 40 are degenerate to within a few MHz. Our predictions of the $D_2{}^{80}Se$ energy spectrum show that for this molecule, the cluster formation is displaced towards higher J values than found for $H_2{}^{80}Se$. The rotational energy level structures in the vibrational ground

states of H_2Se and D_2Se are in qualitative agreement with the predictions of rigid rotor theory at moderate J values. In particular, the four highest energies in each J multiplet form two doublets, and the energy difference between these doublets increases with increasing J. However, when J reaches the so-called critical value J_{CR} this energy difference attains its maximum value. When J increases further the energy difference decreases, and for high J values it tends towards zero so that four-fold clusters are formed. We can say that at $J = J_{CR}$, the qualitative deviation from the usual rigid rotor picture starts. From the MORBID calculations carried out in the present work we determine $J_{CR} \approx 12$ for $H_2{}^{80}Se$ and $J_{CR} \approx 18$ for $D_2{}^{80}Se$, in full agreement with predictions from semiclassical theory.

The analysis of the rotational energy level structure in some excited vibrational states of H_2Se will be reported separately.

II. THE MODEL

The MORBID approach has been extensively described in Refs. (*1, 2*) and we refer the reader to these publications for details. It uses the following expansion for the potential energy function,

$$V(\Delta r_{12}, \Delta r_{32}, \bar{\rho}) = V_0(\bar{\rho}) + \sum_j F_j(\bar{\rho}) y_j + \sum_{j \le k} F_{jk}(\bar{\rho}) y_j y_k + \sum_{j \le k \le m} F_{jkm}(\bar{\rho}) y_j y_k y_m + \sum_{j \le k \le m \le n} F_{jkmn}(\bar{\rho}) y_j y_k y_m y_n, \quad (1)$$

where all of the indices j, k, m, and n assume the values 1 or 3. The quantity y_j in Eq. (1) is given by

$$y_j = 1 - \exp(-a_j \Delta r_{j2}), \quad (2)$$

where the a_j are molecular constants and $\Delta r_{j2} = r_{j2} - r_{j2}^e$, $j = 1$ or 3, is defined as a displacement from the equilibrium value r_{j2}^e of the distance r_{j2} between the "outer" nucleus $j = 1$ or 3 and the "center" nucleus 2. The quantity $\bar{\rho}$ is the instantaneous value of the bond angle supplement (see Fig. 1 of Ref. (*1*)). The $F_{jkm}\ldots$ expansion coefficients of Eq. (1) are functions of $\bar{\rho}$ and are defined as

$$F_j(\bar{\rho}) = \sum_{i=1}^{4} f_j^{(i)} (\cos \rho_e - \cos \bar{\rho})^i, \quad (3)$$

and

$$F_{jk}\ldots(\bar{\rho}) = f_{jk}^{(0)}\ldots + \sum_{i=1}^{N} f_{jk}^{(i)}\ldots (\cos \rho_e - \cos \bar{\rho})^i. \quad (4)$$

The function $F_{jk}(\bar{\rho})$ has $N = 3$, $F_{jkl}(\bar{\rho})$ has $N = 2$, and $F_{jklm}(\bar{\rho})$ has $N = 1$. The function $V_0(\bar{\rho})$ is the potential energy for the molecule bending with bond lengths fixed at their equilibrium values, and here we parameterize it as

$$V_0(\bar{\rho}) = \sum_{i=2}^{8} f_0^{(i)} (\cos \rho_e - \cos \bar{\rho})^i. \quad (5)$$

For a potential energy function with a single minimum, this analytical expression has a physically reasonable asymptotic behavior at all coordinate boundaries: at $\bar{\rho} = 0$ and $\bar{\rho} = \pi$ it has zero slope for all values of r_{12} and r_{32}, at large bond length values it approaches a constant for any value of $\bar{\rho}$, and at short bond lengths it approaches a very large (although not infinite) value.

In the MORBID approach we take the rotation–vibration Hamiltonian to be the sum of the potential energy function given in Eq. (1) and an approximate kinetic energy operator obtained as a fourth-order expansion in the y_j's and in the conjugate momenta $\hat{P}_j = -i\hbar\,\partial/\partial\Delta r_{j2}$. With the MORBID computer program we can in principle calculate all eigenvalues of this Hamiltonian. The calculation proceeds as follows:

(1) We first obtain the eigenfunctions $|N_{\text{vib}}\Gamma_{\text{Sym}}\rangle$ of the Hamiltonian $\hat{H}_{\text{Stretch}}$ [Eq. (58) of Ref. (*1*)] which describes the molecule in question stretching with its bond angle fixed at the equilibrium value α_e. The index N_{vib} characterizes the zeroth-order stretching state, and Γ_{Sym} is the irreducible representation spanned by the function $|N_{\text{vib}}\Gamma_{\text{Sym}}\rangle$ in the appropriate molecular symmetry group.

(2) We then obtain the bending basis functions $|v_2, K\rangle$ [see Section V of Ref. (*1*)] as eigenfunctions for the Hamiltonian $\hat{H}_{\text{Bend}}$ [Eq. (63) of Ref. (*1*)] describing the molecule bending and rotating around the molecule's fixed z-axis [see Ref. (*1*)] with its bond lengths fixed at the equilibrium values r_{12}^e and r_{32}^e. The quantity v_2 is the bending quantum number for a bent triatomic molecule.

(3) We use the products $|N_{\text{vib}}\Gamma_{\text{Sym}}\rangle\,|v_2, K\rangle$ as vibrational basis functions for constructing a matrix representation of the rotation–vibration Hamiltonian for the "complete" molecule and consequently the wavefunction for a rotation–vibration eigenstate of the molecule (which we label by a running index i and by Γ_{rv}, the symmetry of the wavefunction) is given by

$$|i;\,\Gamma_{rv}\rangle = \sum_{N_{\text{vib}},\Gamma_{\text{Sym}},v_2} \sum_{K=0}^{J} c^{(i;\Gamma_{rv})}_{N_{\text{vib}},\Gamma_{\text{Sym}},v_2,K}\,|N_{\text{vib}}\Gamma_{\text{Sym}}\rangle|v_2, K\rangle|J, K, M, \tau\rangle, \tag{6}$$

where $|J, K, M, \tau\rangle$ is a symmetrized rigid rotor eigenfunction defined by Eq. (7.1) of Ref. (*19*):

$$|J, K, M, \tau\rangle = 1/\sqrt{2}(|J, K, M\rangle + (-1)^{J+K+\tau}|J, -K, M\rangle);$$
$$K > 0;\ \tau = 0 \text{ or } 1, \tag{7}$$

and

$$|J, 0, M, \tau_0\rangle = |J, 0, M\rangle, \tag{8}$$

where $\tau_0 = 0$ for J even and $\tau_0 = 1$ for J odd. The expansion coefficients $c^{(i;\Gamma_{rv})}_{N_{\text{vib}},\Gamma_{\text{Sym}},v_2,K}$ in Eq. (6) are determined through matrix diagonalization. The symmetrized stretching function $|N_{\text{vib}}\Gamma_{\text{Sym}}\rangle$ is given by

$$|N_{\text{vib}}\Gamma_{\text{Sym}}\rangle = 1/\sqrt{2}(|n_1n_3\rangle \pm |n_3n_1\rangle); \qquad n_1 \neq n_3, \tag{9}$$

where the plus sign produces a function with $\Gamma_{\text{Sym}} = A_1$ and the minus sign a function with $\Gamma_{\text{Sym}} = B_2$, or

$$|N_{\text{vib}}A_1\rangle = |nn\rangle; \qquad n_1 = n_3 = n. \tag{10}$$

In Eqs. (9) and (10), $|n_1n_3\rangle$ is a product of two Morse oscillator eigenfunctions [Ref. (*1*)]. In the present work we carry out analyses of MORBID eigenfunctions and of so-called localized wavefunctions which can be expressed as linear combinations of the MORBID eigenfunctions (see below). The localized wavefunctions arise naturally in semiclassical theory (*5, 6, 7, 8, 29*). In contrast to the MORBID wavefunctions $|i;\,\Gamma_{rv}\rangle$ the localized functions do not have defined symmetries in the molecular symmetry group. For the analysis of these functions we have found it convenient to express them

(and the MORBID eigenfunctions) as expansions in unsymmetrized, "primitive" basis functions, $|n_1n_3\rangle|v_2, |k|\rangle |J, k, M\rangle$, $-J \leq k \leq J$. Clearly it is straightforward to obtain such an expansion from Eqs. (6)–(10).

III. THE FITTING

The amount of experimental data available for H_2Se and its isotopic species is rather limited. Some of the data (*20, 21*) were measured more than 30 years ago, and the resolution attained in these studies is low compared to present-day standards. More recently, high-resolution studies of the infrared absorption spectrum of hydrogen selenide have been carried out by Edwards and co-workers (*22–26*): they analyzed the ν_1, ν_3, and $2\nu_2$ bands of H_2Se (*22, 25*), the ν_2 band of H_2Se (*23, 26*), and the $2\nu_1$ band of HDSe (*24*). The microwave spectrum of H_2Se has been studied by Helminger and De Lucia (*27*), and experimental investigations of the pure rotational spectrum in the vibrational ground state have recently been reported in Refs. (*9–11*). These high-resolution studies have provided us with highly precise input data for our fitting. In the construction of the input data points, we followed the strategy used in the water fitting of Ref. (*18*): for the isotopic molecules $H_2{}^{80}Se$ and $D_2{}^{80}Se$ we enter for each vibrational state the term value [relative to the $(v_1, v_2, v_3, J_{K_aK_c}) = (0, 0, 0)\ 0_{00}$ state of the isotopic molecule in question] of the lowest measured rotation–vibration state together with the rotational spacings up to $J = 5$ (see Table I). For the excited vibrational states of $H_2{}^{80}Se$ no published rotational term values were available. We constructed such term values by adding ground state term values [determined from the available rotational spectra (*9, 10, 11, 27*)] to the published transition wavenumbers. For $HD^{80}Se$ (*24*), we used the observed wavenumbers for transitions between states with $J \leq 3$ as input data. We did not use input data from isotopic species involving selenium isotopes other than ^{80}Se. Owing to the small relative mass difference between these isotopes, we do not expect that the inclusion of such data will supply information which is not already present in the $H_2{}^{80}Se$ data. The input data set used for the fitting comprised a total of 303 data points.

In the energy calculations carried out during the least-squares fitting, we used the following basis sets:

(1) For $H_2{}^{80}Se$, we calculated the vibrational ($J = 0$) energy spacings with a basis set in which the stretching problem was prediagonalized [see Ref. (*1*)] with Morse oscillator functions $|n_1n_3\rangle$ having $n_1 + n_3 \leq N_{\text{Stretch}} = 12$. In constructing the final rotation–vibration matrices we used the $N_{\text{Bend}} = 13$ lowest bending basis functions, the $N_A = 25$ lowest stretching basis functions of A_1 symmetry, and the $N_B = 20$ lowest stretching basis functions of B_2 symmetry. The rotational spacings were calculated with a basis set having $N_{\text{Stretch}} = 5$, $N_{\text{Bend}} = 8$, and $(N_A, N_B) = (6, 4)$.

(2) For $D_2{}^{80}Se$, the vibrational ($J = 0$) energy spacings were calculated with a basis set defined by $N_{\text{Stretch}} = 12$, $N_{\text{Bend}} = 9$, and $(N_A, N_B) = (9, 6)$. The basis set used for the rotational spacings had $N_{\text{Stretch}} = 5$, $N_{\text{Bend}} = 6$, and $(N_A, N_B) = (4, 2)$.

(3) Finally for $HD^{80}Se$, we calculated the rotation–vibration spacings used as input with the basis set $N_{\text{Stretch}} = 21$, $N_{\text{Bend}} = 11$, and $N_A = 21$.

In order to obtain a set of initial parameter values with which to start the fitting procedure, we estimated the parameters of Eqs. (1)–(4) on the basis of the results obtained by Kauppi and Halonen (*17*). Their parameterization of the potential energy

TABLE I

Observed and Calculated Vibrational and Rotational Term Values (cm^{-1}) for Hydrogen Selenide

(v_1, v_2, v_3)	$J'_{K'_a K'_c} - J''_{K''_a K''_c}$	obs.[a] cm^{-1}	o.−c. cm^{-1}	weight	(v_1, v_2, v_3)	$J'_{K'_a K'_c} - J''_{K''_a K''_c}$	obs.[a] cm^{-1}	o.−c. cm^{-1}	weight
$H_2^{80}Se$									
(0,0,0)[b]	0_{00}	0.0			(0,2,0)[d]	0_{00}	2059.96680	−0.00965	10.0
	$1_{01}-0_{00}$	11.62634	−0.00045	100.0		$1_{01}-0_{00}$	11.905	−0.003	10.0
	$1_{11}-0_{00}$	12.07099	0.00021	100.0		$1_{11}-0_{00}$	12.491	−0.004	10.0
	$1_{10}-0_{00}$	15.89508	−0.00011	100.0		$1_{10}-0_{00}$	16.782	−0.002	10.0
	$2_{02}-0_{00}$	31.45436	−0.00037	100.0		$2_{02}-0_{00}$	31.954	0.000	10.0
	$2_{12}-0_{00}$	31.50012	−0.00040	100.0		$2_{12}-0_{00}$	32.022	−0.001	10.0
	$2_{11}-0_{00}$	42.96076	−0.00133	100.0		$2_{11}-0_{00}$	44.876	0.001	10.0
	$2_{21}-0_{00}$	44.29109	0.00057	100.0		$2_{21}-0_{00}$	46.622	−0.007	10.0
	$2_{20}-0_{00}$	47.70311	−0.00038	100.0		$2_{20}-0_{00}$	50.365	−0.018	10.0
	$3_{03}-0_{00}$	58.91334	−0.00061	100.0		$3_{03}-0_{00}$	59.405	0.001	10.0
	$3_{13}-0_{00}$	58.91713	−0.00063	100.0		$3_{13}-0_{00}$	59.405	−0.005	10.0
	$3_{12}-0_{00}$	78.93797	−0.00076	100.0		$3_{12}-0_{00}$	82.010	0.002	10.0
	$3_{22}-0_{00}$	79.16368	−0.00094	100.0		$3_{22}-0_{00}$	82.341	−0.006	10.0
	$3_{21}-0_{00}$	89.94535	−0.00283	100.0		$3_{21}-0_{00}$	94.307	0.001	10.0
	$3_{31}-0_{00}$	92.59144	0.00069	100.0		$3_{31}-0_{00}$	97.771	−0.018	10.0
	$3_{30}-0_{00}$	95.45717	−0.00090	100.0		$3_{30}-0_{00}$	100.837	−0.011	10.0
	$4_{04}-0_{00}$	94.14466	−0.00080	100.0		$4_{04}-0_{00}$	94.432	−0.000	1.0
	$4_{14}-0_{00}$	94.14499	−0.00080	100.0		$4_{14}-0_{00}$	94.432	−0.001	1.0
	$4_{13}-0_{00}$	122.32621	−0.00074	100.0		$4_{13}-0_{00}$	126.350	0.051	1.0
	$4_{23}-0_{00}$	122.35240	−0.00086	100.0		$4_{23}-0_{00}$	126.350	0.006	1.0
	$4_{22}-0_{00}$	142.01880	−0.00190	100.0		$4_{22}-0_{00}$	148.422	0.008	1.0
	$4_{32}-0_{00}$	142.67847	−0.00261	100.0		$4_{32}-0_{00}$	149.387	−0.011	1.0
	$4_{31}-0_{00}$	152.56490	−0.00523	100.0		$4_{31}-0_{00}$	160.182	−0.004	1.0
	$4_{41}-0_{00}$	156.93151	0.00008	100.0		$4_{41}-0_{00}$	165.889	−0.028	1.0
	$4_{40}-0_{00}$	159.19537	−0.00197	100.0		$4_{40}-0_{00}$	168.218	−0.021	1.0
	$5_{05}-0_{00}$	137.16228	−0.00087	100.0		$5_{05}-0_{00}$	137.066	0.004	1.0
	$5_{15}-0_{00}$	137.16231	−0.00087	100.0		$5_{15}-0_{00}$	137.066	0.004	1.0
	$5_{14}-0_{00}$	173.39399	−0.00028	100.0		$5_{14}-0_{00}$	178.060	0.020	1.0
	$5_{24}-0_{00}$	173.39691	−0.00031	100.0		$5_{24}-0_{00}$	178.075	0.029	1.0
	$5_{23}-0_{00}$	201.39609	−0.00196	100.0		$5_{23}-0_{00}$	209.647	0.017	1.0
	$5_{33}-0_{00}$	201.49905	−0.00250	100.0		$5_{33}-0_{00}$	209.813	0.008	1.0
	$5_{32}-0_{00}$	220.53802	−0.00413	100.0		$5_{32}-0_{00}$	230.981	0.022	1.0
	$5_{42}-0_{00}$	222.01235	−0.00622	100.0		$5_{42}-0_{00}$	233.108	−0.022	1.0
	$5_{41}-0_{00}$	230.80795	−0.00899	100.0		$5_{41}-0_{00}$	242.501	−0.008	1.0
	$5_{51}-0_{00}$	237.25049	−0.00191	100.0		$5_{51}-0_{00}$	250.874	−0.050	1.0
	$5_{50}-0_{00}$	238.93873	−0.00410	100.0		$5_{50}-0_{00}$	252.540	−0.036	1.0
(0,1,0)[c]	0_{00}	1034.16520	0.01398	10.0	(1,0,0)[d]	0_{00}	2344.36240	−0.00856	10.0
	$1_{01}-0_{00}$	11.75991	−0.00115	10.0		$1_{01}-0_{00}$	11.456	0.006	10.0
	$1_{11}-0_{00}$	12.27415	0.00147	10.0		$1_{11}-0_{00}$	11.896	0.002	10.0
	$1_{10}-0_{00}$	16.32380	0.00033	10.0		$1_{10}-0_{00}$	15.669	0.006	10.0
	$2_{02}-0_{00}$	31.68876	0.00028	10.0		$2_{02}-0_{00}$	31.036	0.052	10.0
	$2_{12}-0_{00}$	31.74526	0.00035	10.0		$2_{12}-0_{00}$	31.036	0.011	10.0
	$2_{11}-0_{00}$	43.88051	−0.00306	10.0		$2_{11}-0_{00}$	42.343	0.029	10.0
	$2_{21}-0_{00}$	45.41841	0.00468	10.0		$2_{21}-0_{00}$	43.654	0.013	10.0
	$2_{20}-0_{00}$	48.99469	0.00101	10.0		$2_{20}-0_{00}$	47.075	0.009	10.0
	$3_{03}-0_{00}$	59.13563	0.00132	10.0		$3_{03}-0_{00}$	58.058	0.031	10.0
	$3_{13}-0_{00}$	59.14058	0.00128	10.0		$3_{13}-0_{00}$	58.058	0.028	10.0
	$3_{12}-0_{00}$	80.41393	0.00109	10.0		$3_{12}-0_{00}$	77.807	0.037	10.0
	$3_{22}-0_{00}$	80.69202	0.00135	10.0		$3_{22}-0_{00}$	78.021	0.050	10.0
	$3_{21}-0_{00}$	92.04265	−0.00656	10.0		$3_{21}-0_{00}$	88.652	0.057	10.0
	$3_{31}-0_{00}$	95.09913	0.00854	10.0		$3_{31}-0_{00}$	91.248	0.026	10.0
	$3_{30}-0_{00}$	98.05544	0.00205	10.0		$3_{30}-0_{00}$	94.330	0.002	10.0
	$4_{04}-0_{00}$	94.25911	0.00337	10.0		$4_{04}-0_{00}$	92.772	0.048	1.0
	$4_{14}-0_{00}$	94.25956	0.00336	10.0		$4_{14}-0_{00}$	92.772	0.047	1.0
	$4_{13}-0_{00}$	124.23179	0.00511	10.0		$4_{13}-0_{00}$	120.558	0.058	1.0
	$4_{23}-0_{00}$	124.26597	0.00484	10.0		$4_{23}-0_{00}$	120.573	0.053	1.0
	$4_{22}-0_{00}$	145.10092	−0.00036	10.0		$4_{22}-0_{00}$	140.001	0.073	1.0
	$4_{32}-0_{00}$	145.91019	0.00007	10.0		$4_{32}-0_{00}$	140.580	0.064	1.0
	$4_{31}-0_{00}$	156.23069	−0.01247	10.0		$4_{31}-0_{00}$	150.371	0.084	1.0
	$4_{41}-0_{00}$	161.26733	0.01188	10.0		$4_{41}-0_{00}$	154.632	0.065	1.0
	$4_{40}-0_{00}$	163.55370	0.00315	10.0		$4_{40}-0_{00}$	157.497	−0.023	1.0
	$5_{05}-0_{00}$	137.07768	0.00696	10.0		$5_{05}-0_{00}$	135.145	0.055	1.0
	$5_{15}-0_{00}$	137.07772	0.00696	10.0		$5_{15}-0_{00}$	135.145	0.055	1.0
	$5_{14}-0_{00}$	175.61828	0.01215	10.0		$5_{14}-0_{00}$	170.886	0.089	1.0
	$5_{24}-0_{00}$	175.62229	0.01206	10.0		$5_{24}-0_{00}$	170.892	0.094	1.0
	$5_{23}-0_{00}$	205.36146	0.00643	10.0		$5_{23}-0_{00}$	198.483	0.081	1.0
	$5_{33}-0_{00}$	205.49543	0.00530	10.0		$5_{33}-0_{00}$	198.574	0.093	1.0
	$5_{32}-0_{00}$	225.56415	−0.00557	10.0		$5_{32}-0_{00}$	217.414	0.116	1.0
	$5_{42}-0_{00}$	227.36096	−0.00577	10.0		$5_{42}-0_{00}$	218.717	0.107	1.0
	$5_{41}-0_{00}$	236.43514	−0.02205	10.0		$5_{41}-0_{00}$	227.526	0.124	1.0
	$5_{51}-0_{00}$	243.84908	0.01311	10.0		$5_{51}-0_{00}$	233.628	0.093	1.0
	$5_{50}-0_{00}$	245.51173	0.00333	10.0		$5_{50}-0_{00}$	236.566	−0.055	1.0
(0,0,1)[d]	0_{00}	2357.6619	0.0663	10.0		$3_{03}-0_{00}$	58.180	0.020	10.0
	$1_{11}-0_{00}$	11.868	0.006	10.0		$3_{13}-0_{00}$	58.178	0.019	10.0
	$1_{10}-0_{00}$	15.658	−0.002	10.0		$3_{12}-0_{00}$	77.894	0.009	10.0
	$2_{02}-0_{00}$	31.059	0.005	10.0		$3_{22}-0_{00}$	77.848	0.061	10.0
	$2_{12}-0_{00}$	31.048	0.019	10.0		$3_{21}-0_{00}$	89.010	0.080	10.0
	$2_{20}-0_{00}$	47.000	0.011	10.0		$3_{31}-0_{00}$	90.903	−0.094	10.0

TABLE I—*Continued*

(v_1, v_2, v_3)	$J'_{K'_a K'_c} - J''_{K''_a K''_c}$	obs.[a] cm^{-1}	o.−c. cm^{-1}	weight	(v_1, v_2, v_3)	$J'_{K'_a K'_c} - J''_{K''_a K''_c}$	obs.[a] cm^{-1}	o.−c. cm^{-1}	weight
(0,0,1)[d]	$4_{04} - 0_{00}$	93.009	0.047	1.0		$5_{42} - 0_{00}$	217.934	0.277	1.0
	$4_{14} - 0_{00}$	93.009	0.047	1.0		$5_{41} - 0_{00}$	228.597	0.200	1.0
	$4_{13} - 0_{00}$	120.687	0.050	1.0		$5_{51} - 0_{00}$	233.006	−0.221	1.0
	$4_{23} - 0_{00}$	120.688	0.055	1.0	(1,1,0)[e]	0_{00}	3361.72	0.39	1.0
	$4_{22} - 0_{00}$	140.165	0.017	1.0	(0,1,1)[e]	0_{00}	3371.81	0.30	1.0
	$4_{32} - 0_{00}$	140.136	0.147	1.0	(2,0,0)[e]	0_{00}	4615.33	−0.05	1.0
	$5_{05} - 0_{00}$	135.525	0.062	1.0	(1,0,1)[e]	0_{00}	4617.40	−0.21	1.0
	$5_{15} - 0_{00}$	135.525	0.062	1.0	(2,1,0)[e]	0_{00}	5612.73	−0.09	1.0
	$5_{14} - 0_{00}$	171.123	0.086	1.0	(1,1,1)[e]	0_{00}	5613.72	−0.32	1.0
	$5_{24} - 0_{00}$	171.093	0.056	1.0	(1,0,2)[e]	0_{00}	6798.15	0.05	1.0
	$5_{23} - 0_{00}$	198.632	0.079	1.0	(2,0,1)[e]	0_{00}	6798.23	−0.03	1.0
	$5_{33} - 0_{00}$	198.633	0.094	1.0	(3,0,0)[e]	0_{00}	6953.6	0.3	0.1
	$5_{32} - 0_{00}$	217.753	0.033	1.0	(3,0,1)[e]	0_{00}	8894.6	0.6	0.1
$D_2^{80}Se$									
(0,0,0)[f]	0_{00}	0.0				$3_{31} - 0_{00}$	48.38	0.22	1.0
	$1_{01} - 0_{00}$	5.85	−0.00	1.0		$3_{30} - 0_{00}$	49.48	0.05	1.0
	$1_{11} - 0_{00}$	6.18	0.00	1.0		$4_{04} - 0_{00}$	47.97	0.08	0.1
	$1_{10} - 0_{00}$	8.06	0.00	1.0		$4_{14} - 0_{00}$	47.97	0.08	0.1
	$2_{02} - 0_{00}$	15.97	0.01	1.0		$4_{13} - 0_{00}$	62.78	0.06	0.1
	$2_{12} - 0_{00}$	16.01	0.01	1.0		$4_{23} - 0_{00}$	62.78	0.03	0.1
	$2_{11} - 0_{00}$	21.65	0.01	1.0		$4_{22} - 0_{00}$	73.00	0.08	0.1
	$2_{21} - 0_{00}$	22.63	0.02	1.0		$4_{32} - 0_{00}$	73.77	0.22	0.1
	$2_{20} - 0_{00}$	24.22	0.02	1.0		$4_{31} - 0_{00}$	78.30	0.02	0.1
	$3_{03} - 0_{00}$	29.95	0.02	1.0		$4_{40} - 0_{00}$	82.73	0.13	0.1
	$3_{13} - 0_{00}$	29.95	0.02	1.0		$5_{05} - 0_{00}$	69.81	0.11	0.1
	$3_{12} - 0_{00}$	40.00	0.03	1.0		$5_{15} - 0_{00}$	69.81	0.11	0.1
	$3_{22} - 0_{00}$	40.19	0.02	1.0		$5_{14} - 0_{00}$	88.90	0.11	0.1
	$3_{21} - 0_{00}$	45.37	0.03	1.0		$5_{24} - 0_{00}$	88.90	0.10	0.1
	$3_{31} - 0_{00}$	47.32	0.05	1.0		$5_{23} - 0_{00}$	103.69	0.18	0.1
	$3_{30} - 0_{00}$	48.55	0.04	1.0		$5_{33} - 0_{00}$	103.78	0.16	0.1
	$4_{04} - 0_{00}$	47.88	0.03	0.1		$5_{42} - 0_{00}$	114.80	0.18	0.1
	$4_{14} - 0_{00}$	47.88	0.03	0.1	(1,0,0)[f]	0_{00}	1686.70	−0.33	1.0
	$4_{13} - 0_{00}$	62.10	0.05	0.1		$1_{11} - 0_{00}$	6.12	0.00	1.0
	$4_{23} - 0_{00}$	62.12	0.05	0.1		$2_{02} - 0_{00}$	15.78	−0.01	1.0
	$4_{22} - 0_{00}$	71.91	0.08	0.1		$2_{20} - 0_{00}$	23.99	0.04	1.0
	$4_{32} - 0_{00}$	72.46	0.06	0.1		$3_{03} - 0_{00}$	29.59	−0.03	1.0
	$4_{31} - 0_{00}$	77.05	0.08	0.1		$4_{04} - 0_{00}$	47.37	0.02	1.0
	$4_{41} - 0_{00}$	80.28	0.12	0.1		$4_{40} - 0_{00}$	80.10	−0.01	1.0
	$4_{40} - 0_{00}$	81.15	0.11	0.1		$5_{05} - 0_{00}$	69.04	0.02	1.0
	$5_{05} - 0_{00}$	69.79	0.05	0.1		$5_{15} - 0_{00}$	69.04	0.02	1.0
	$5_{15} - 0_{00}$	69.79	0.05	0.1		$5_{41} - 0_{00}$	111.70	−0.18	1.0
	$5_{14} - 0_{00}$	88.10	0.09	0.1	(0,0,1)[f]	0_{00}	1697.36	−0.45	1.0
	$5_{24} - 0_{00}$	88.10	0.08	0.1		$1_{01} - 0_{00}$	5.74	−0.07	1.0
	$5_{23} - 0_{00}$	102.24	0.14	0.1		$1_{10} - 0_{00}$	8.06	0.09	1.0
	$5_{33} - 0_{00}$	102.32	0.12	0.1		$2_{02} - 0_{00}$	15.92	0.10	1.0
	$5_{32} - 0_{00}$	111.66	0.19	0.1		$2_{12} - 0_{00}$	15.96	0.10	1.0
	$5_{42} - 0_{00}$	112.85	0.13	0.1		$2_{21} - 0_{00}$	22.53	0.20	1.0
	$5_{41} - 0_{00}$	116.74	0.17	0.1		$2_{20} - 0_{00}$	23.92	−0.02	1.0
	$5_{51} - 0_{00}$	121.54	0.25	0.1		$3_{03} - 0_{00}$	29.69	0.03	1.0
	$5_{50} - 0_{00}$	122.11	0.25	0.1		$3_{13} - 0_{00}$	29.69	0.03	1.0
(0,1,0)[f]	0_{00}	741.42	−0.38	1.0		$3_{21} - 0_{00}$	44.93	−0.03	1.0
	$1_{01} - 0_{00}$	5.88	−0.02	1.0		$3_{30} - 0_{00}$	48.08	0.11	1.0
	$1_{11} - 0_{00}$	6.25	0.00	1.0		$4_{04} - 0_{00}$	47.47	0.04	0.1
	$1_{10} - 0_{00}$	8.14	−0.07	1.0		$4_{14} - 0_{00}$	47.47	0.04	0.1
	$2_{02} - 0_{00}$	16.06	0.02	1.0		$4_{32} - 0_{00}$	71.97	0.20	0.1
	$2_{12} - 0_{00}$	16.10	0.01	1.0		$4_{31} - 0_{00}$	76.24	−0.09	0.1
	$2_{11} - 0_{00}$	21.97	0.00	1.0		$4_{41} - 0_{00}$	79.40	0.24	0.1
	$2_{21} - 0_{00}$	23.05	0.04	1.0		$4_{40} - 0_{00}$	80.41	0.31	0.1
	$2_{20} - 0_{00}$	24.65	−0.01	1.0		$5_{05} - 0_{00}$	69.29	0.16	0.1
	$3_{03} - 0_{00}$	30.05	0.04	1.0		$5_{15} - 0_{00}$	69.29	0.16	0.1
	$3_{13} - 0_{00}$	30.05	0.04	1.0		$5_{23} - 0_{00}$	101.27	0.16	0.1
	$3_{12} - 0_{00}$	40.34	−0.15	1.0		$5_{32} - 0_{00}$	110.60	0.10	0.1
	$3_{22} - 0_{00}$	40.78	0.07	1.0		$5_{41} - 0_{00}$	115.74	0.14	0.1
	$3_{21} - 0_{00}$	46.07	−0.01	1.0		$5_{50} - 0_{00}$	120.67	0.26	0.1
$HD^{80}Se$									
(2,0,0)[g]	0_{00}	4617.89230	−0.04361	10.0		$1_{01} - 1_{10}$	4612.526	−0.038	10.0
	$2_{20} - 3_{31}$	4573.183	0.021	10.0		$1_{10} - 1_{01}$	4622.758	−0.028	10.0
	$2_{11} - 3_{22}$	4585.661	−0.019	10.0		$2_{02} - 1_{11}$	4626.756	−0.026	10.0
	$1_{11} - 2_{20}$	4589.229	−0.024	10.0		$3_{12} - 3_{03}$	4627.271	0.005	10.0
	$1_{10} - 2_{21}$	4590.951	−0.037	10.0		$3_{21} - 3_{12}$	4627.485	0.031	10.0
	$3_{22} - 3_{31}$	4592.613	0.041	10.0		$3_{13} - 2_{02}$	4637.551	−0.008	10.0
	$2_{02} - 3_{13}$	4597.149	−0.028	10.0		$2_{20} - 1_{11}$	4644.261	0.015	10.0
	$2_{12} - 2_{21}$	4601.291	−0.026	10.0		$3_{22} - 2_{11}$	4647.612	0.020	10.0
	$2_{12} - 3_{03}$	4601.291	−0.019	10.0		$3_{21} - 2_{12}$	4653.444	0.038	10.0
	$2_{11} - 2_{20}$	4605.284	−0.018	10.0		$3_{31} - 2_{20}$	4656.724	0.105	10.0
	$1_{11} - 2_{02}$	4608.338	−0.024	10.0		$3_{30} - 2_{21}$	4657.071	0.090	10.0
	$2_{02} - 2_{11}$	4610.691	−0.028	10.0					

[a] Experimental energy spacings. Data labeled by (v_1, v_2, v_3) 0_{00} are vibrational term values measured relative to the (0, 0, 0) 0_{00} level of the isotopic molecule in question. Unless otherwise indicated, the other data are spacings within the particular (v_1, v_2, v_3) state.

[b] Ref. (*11*). [c] Refs. (*23, 26*). [d] Refs. (*22, 25*). [e] Ref. (*21*). [f] Ref. (*20*).

[g] Ref. (*24*). The datum labeled by (2, 0, 0) 0_{00} is the $2\nu_1$ vibrational term value of $HD^{80}Se$ measured relative to the (0, 0, 0) 0_{00} level of this molecule. The other data are measured transition wavenumbers in the $2\nu_1$ band.

function differs from ours in that they express the dependence on the bending angle $\bar{\rho}$ as an expansion in $\rho_e - \bar{\rho}$, whereas we employ an expansion in $\cos \rho_e - \cos \bar{\rho}$. By expressing $\rho_e - \bar{\rho}$ as a fourth-order Taylor expansion in $\cos \rho_e - \cos \bar{\rho}$, we could transform their parameters to the values required by our analytical expression for $V(\Delta r_{12}, \Delta r_{32}, \bar{\rho})$ [Eq. (1)]. In the fitting, we could usefully vary 14 parameters. One parameter, a_1 [Eq. (2)], was found to be strongly correlated to the $f_{11}^{(0)}$ parameter. This correlation is caused by the lack of highly excited stretching states in the input data. Consequently we constrained a_1 to the value determined by Kauppi and Halonen (*17*). This value is in keeping with the ab initio value (*15*) so that it probably represents a rather realistic estimate of a_1. The residuals (observed − calculated) are given in Table I. The input data are reproduced with an RMS deviation of 0.0975 cm^{-1} for the rotational energy spacings and 0.268 cm^{-1} for the vibrational spacings. The fitted parameter values are presented in Table II, and Fig. 1 shows graphical representations of sections of the fitted surface.

Further, we have obtained the values of the first to fourth derivatives at equilibrium ($\Delta r_{12} = \Delta r_{32} = 0, \bar{\rho} = \rho_e$) of the potential energy function given by Eqs. (1)–(4) from the parameter values of Table II. We define these "force constants" as the derivatives of $V(\Delta r_{12}, \Delta r_{32}, \bar{\rho})$ [Eq. (1)] at equilibrium, e.g.,

$$f_{rr} = \left(\frac{\partial^2 V}{\partial \Delta r_{12}^2}\right)_e, \tag{11}$$

$$f_{r\alpha} = \left(\frac{\partial^2 V}{\partial \Delta r_{12} \partial \alpha}\right)_e, \tag{12}$$

etc., $\alpha = \pi - \bar{\rho}$ being the bond angle. The resulting values are given in Table III which also contains the force constant values obtained ab initio by Senekowitsch *et al.* (*15*) and those obtained by Kauppi and Halonen (*17*).

To investigate the predictive power of the optimized parameters we have calculated an extensive set of rotational energy levels in the vibrational ground state of $H_2{}^{80}Se$ (for $J = 0$ through 40) and compared them with the values derived from experiment (*11*) which are available up to $J = 23$. These predictions were made with a basis set defined by $N_{\text{Stretch}} = 5$, $N_{\text{Bend}} = 8$, and $(N_A, N_B) = (6, 4)$. Only very few transitions

TABLE II

Fitted Potential Energy Parameters for Hydrogen Selenide

ρ_e/deg	89.079336(137)[a]		
r_{12}^e/Å	1.4591785(171)		
a_1/Å^{-1}	1.6657[b]		
$f_0^{(2)}$/cm^{-1}	17758.37(766)	$f_1^{(1)}$/cm^{-1}	−2056.6(925)
$f_0^{(3)}$/cm^{-1}	957.3(366)	$f_1^{(2)}$/cm^{-1}	−5264.2(785)
$f_0^{(4)}$/cm^{-1}	4916.6(265)	$f_{13}^{(0)}$/cm^{-1}	−405.23(316)
$f_{11}^{(0)}$/cm^{-1}	31807.21(179)	$f_{13}^{(1)}$/cm^{-1}	4874.(256)
$f_{11}^{(2)}$/cm^{-1}	−5037.4(946)	$f_{13}^{(2)}$/cm^{-1}	3108.(131)
$f_{113}^{(0)}$/cm^{-1}	−250.8(253)	$f_{1111}^{(0)}$/cm^{-1}	2373.86(763)

[a] Quantities in parentheses are standard errors in units of the last digit given.
[b] Taken from Ref. (*17*).

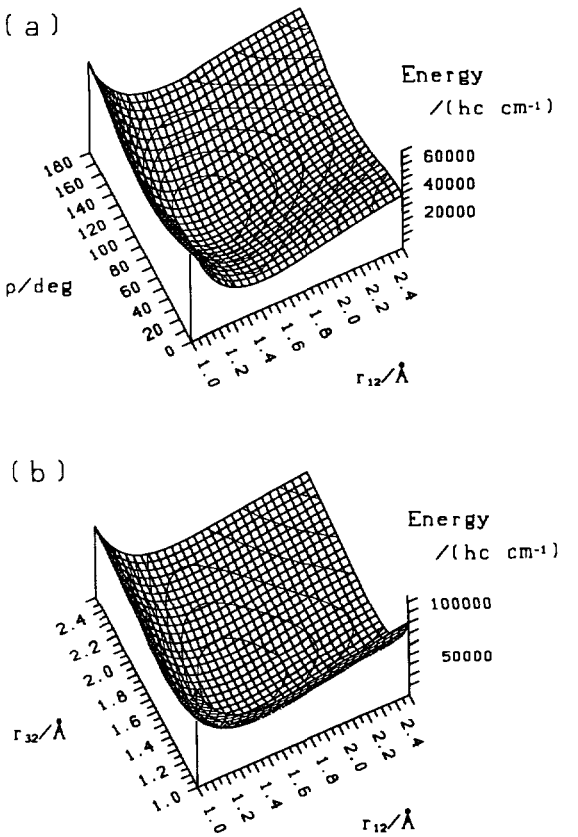

FIG. 1. Sections of the fitted potential energy surface. (a) V is shown as a function of the angle $\rho = \pi - \alpha$, where α is the bond angle, and the bond distance r_{12}. (b) V is shown as a function of the bond distances r_{12} and r_{32}. On both plots, contour lines are drawn at intervals of 5000 cm^{-1} above the minimum energy.

involving $J > 20$ have been observed, whereas for $J \leq 20$, experiment yields a rather complete set of rotational energy levels in the vibrational ground state. The MORBID calculation reproduces these $J \leq 20$ energy levels with an RMS deviation of 0.371 cm^{-1} and the $J = 20$ energy levels with an RMS deviation of 0.783 cm^{-1}. The fitted rotational energy spacings in the vibrational ground state of $H_2{}^{80}Se$ ($J \leq 5$) are reproduced with an RMS deviation of 0.0026 cm^{-1}. The observed transition involving the highest J values is $23_{23\,0} \leftarrow 23_{22\,1}$ (*11*); this transition takes place between two states belonging to the same four-fold cluster. Its frequency is observed experimentally as 118.515 GHz (*11*) and the MORBID prediction yields 114 GHz.

As already mentioned, we have taken the prediction of the rotational energy levels in the vibrational ground state to $J = 40$, and Fig. 2 is a term value diagram showing the cluster structure of the rotational energy levels in the vibrational ground state of $H_2{}^{80}Se$. The levels are plotted relative to the highest term value for each J multiplet. The term values calculated by the MORBID program (using the parameters from Table II) are given as horizontal lines, and experimental term values are shown as circles. Filled circles represent term values that were included in the input data for the MORBID fitting ($J \leq 5$); empty circles represent experimental term values which

TABLE III

Equilibrium Geometry and Force Constants for H_2Se

	ab initio	Ref. (17)	This work
r_{12}^e/Å	1.461	1.460	1.459
α_e[a]/deg	90.62	90.57	90.921
f_{rr}/aJ Å^{-2}	3.485	3.501	3.506
$f_{\alpha\alpha}$/aJ	0.760	0.700	0.705
$f_{rr'}$ /aJ Å^{-2}	−0.013	−0.022	−0.045
$f_{r\alpha}$/aJ Å^{-1}	0.075	0.080	0.136
f_{rrr}/aJ Å^{-3}	−17.390	−17.50	−17.520
$f_{\alpha\alpha\alpha}$ /aJ	−0.315	−0.161	−0.148
$f_{rrr'}$/aJ Å^{-3}	−0.019	0.0	−0.027
$f_{rr\alpha}$/aJ Å^{-2}	−0.110	−0.068	−0.340
$f_{rr'\alpha}$/aJ Å^{-2}	−0.220	−0.332	−1.611
$f_{r\alpha\alpha}$/aJ Å^{-1}	−0.355	−0.275	−1.048
f_{rrrr}/aJ Å^{-4}	75.761	76.95	76.808
$f_{\alpha\alpha\alpha\alpha}$/aJ	−1.074	0.0	−0.467
$f_{rrrr'}$/aJ Å^{-4}	−0.133	0.0	0.672
$f_{rrr'r'}$/aJ Å^{-4}	0.356	0.0	0.549
$f_{rrr\alpha}$/aJ Å^{-3}	−0.077	0.0	0.755
$f_{rrr'\alpha}$/aJ Å^{-3}	0.148	0.0	5.369
$f_{rr\alpha\alpha}$/aJ Å^{-2}	−0.646	−0.756	−3.170
$f_{rr'\alpha\alpha}$/aJ Å^{-2}	0.324	0.0	4.162
$f_{r\alpha\alpha\alpha}$ /aJ Å^{-1}	0.184	0.0	−0.205

[a]Equilibrium bond angle.

were not included. At $J = 40$, MORBID predicts that the individual energy levels of the "top" cluster are degenerate to within 3 MHz.

Figure 3 is analogous to Fig. 2, but shows the cluster structure of the rotational energy spectrum in the vibrational ground state of $D_2{}^{80}Se$. The basis set for this calculation was $N_{\text{Stretch}} = 5$, $N_{\text{Bend}} = 8$, and $(N_A, N_B) = (6, 4)$.

Finally, we have used our fitted potential energy surface to calculate an extensive set of vibrational term values for $H_2{}^{80}Se$, $D_2{}^{80}Se$, and $HD^{80}Se$. The results are given in Table IV. The basis sets were $N_{\text{Stretch}} = 12$, $N_{\text{Bend}} = 21$, and $(N_A, N_B) = (25, 20)$ for $H_2{}^{80}Se$, $N_{\text{Stretch}} = 12$, $N_{\text{Bend}} = 22$, and $(N_A, N_B) = (30, 25)$ for $D_2{}^{80}Se$, and $N_{\text{Stretch}} = 12$, $N_{\text{Bend}} = 21$, and $N_A = 55$ for $HD^{80}Se$. Local mode behavior (*3, 4*) is readily recognized in the vibrational energy spectra of $H_2{}^{80}Se$ and $D_2{}^{80}Se$.

It is obvious from Table I that very few experimental data are available for $D_2{}^{80}Se$ and $HD^{80}Se$. We hope that the predictions given in Table IV will encourage further experimental work on these molecules. Predictions of additional energy levels, for example, of the rotational energy level structure in excited vibrational states or of other isotopic species, are available from the authors on request.

IV. DISCUSSION

The force constants determined in the present work (Table III) are in broad agreement with those calculated ab initio by Senekowitsch *et al.* (*15*) and those determined by Kauppi and Halonen (*17*) from a fit to experiment. The deviations between the three sets of force constants are comparable to the analogous deviations for H_2O given in Table V of Ref. (*18*). In that table, force constants determined with the MORBID

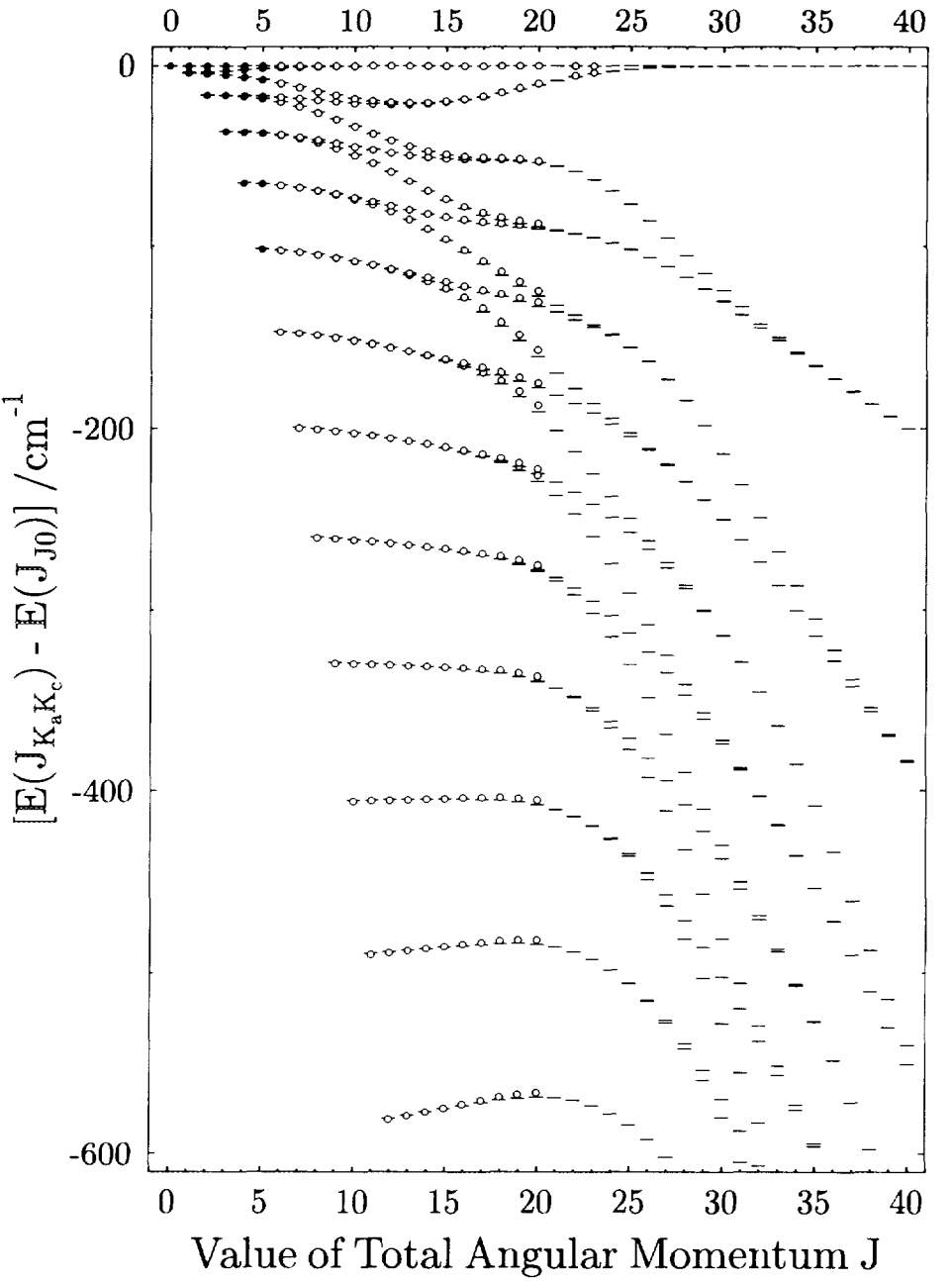

FIG. 2. The rotational energy level structure in the vibrational ground state of $H_2{}^{80}Se$. Term values are plotted relative to the highest term value for each J multiplet. The term values calculated by the MORBID program (using the parameters from Table II) are given as horizontal lines, and experimental term values are shown as circles. Filled circles represent term values that were included in the input data for the MORBID fitting ($J \leq 5$); empty circles represent experimental term values which were not included.

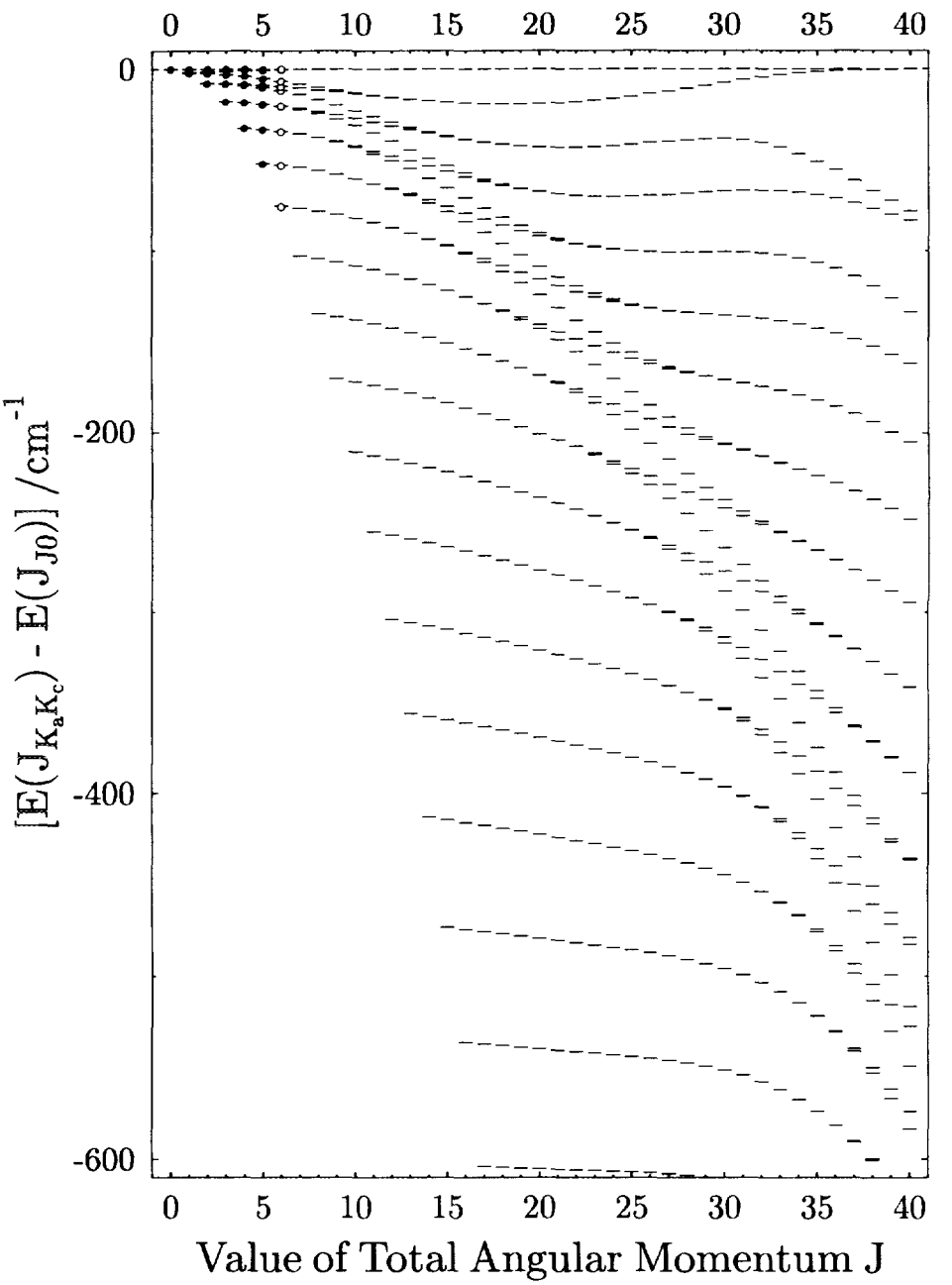

FIG. 3. The rotational energy level structure in the vibrational ground state of $D_2{}^{80}Se$. Term values are plotted relative to the highest term value for each J multiplet. The term values calculated by the MORBID program (using the parameters from Table II) are given as horizontal lines, and experimental term values are shown as circles. Filled circles represent term values that were included in the input data for the MORBID fitting ($J \leq 5$); empty circles represent experimental term values which were not included.

TABLE IV

Calculated Vibrational Levels

$H_2{}^{80}Se$				$D_2{}^{80}Se$				$HD^{80}Se$			
v_1	v_2	v_3	/cm^{-1}	v_1	v_2	v_3	/cm^{-1}	v_1	v_2	v_3	/cm^{-1}
0	1	0	1034.15	0	1	0	741.80	0	1	0	900.51
0	2	0	2059.98	0	2	0	1479.50	0	0	1	1692.02
1	0	0	2344.37	1	0	0	1687.03	0	2	0	1794.67
0	0	1	2357.60	0	0	1	1697.81	1	0	0	2351.14
0	3	0	3076.65	0	3	0	2212.81	0	1	1	2582.68
1	1	0	3361.33	1	1	0	2420.12	0	3	0	2681.94
0	1	1	3371.51	0	1	1	2429.30	1	1	0	3233.08
0	4	0	4083.38	0	4	0	2941.42	0	0	2	3341.40
1	2	0	4370.28	1	2	0	3149.25	0	2	1	3467.13
0	2	1	4377.45	0	2	1	3156.83	0	4	0	3561.81
2	0	0	4615.38	2	0	0	3339.53	1	0	1	4041.37
1	0	1	4617.61	1	0	1	3342.31	1	2	0	4108.96
0	0	2	4702.03	0	0	2	3386.36	0	1	2	4222.34
0	5	0	5079.42	0	5	0	3665.06	0	3	1	4344.83
1	3	0	5370.37	1	3	0	3874.09	0	5	0	4433.79
0	3	1	5374.58	0	3	1	3880.09	2	0	0	4617.93
2	1	0	5612.82	2	1	0	4062.97	1	1	1	4913.06
1	1	1	5614.04	1	1	1	4064.99	0	0	3	4948.01
0	1	2	5698.02	0	1	2	4108.50	1	3	0	4978.22
0	6	0	6064.06	0	6	0	4383.46	0	2	2	5097.21
1	4	0	6360.77	1	4	0	4594.34	0	4	1	5215.26
0	4	1	6362.10	0	4	1	4598.78	0	6	0	5297.40
2	2	0	6602.44	2	2	0	4782.48	2	1	0	5481.31
1	2	1	6602.84	1	2	1	4783.84	1	0	2	5688.56
0	2	2	6686.55	0	2	2	4826.90	1	2	1	5778.88
3	0	0	6798.10	3	0	0	4947.91	0	1	3	5819.63
2	0	1	6798.26	2	0	1	4948.25	1	4	0	5840.34
1	0	2	6953.27	1	0	2	5023.61	0	3	2	5965.46
0	0	3	6977.66	0	0	3	5043.63	0	5	1	6077.93
0	7	0	7036.65	0	7	0	5096.36	0	7	0	6152.18
0	5	1	7339.26	1	5	0	5309.70	2	0	1	6306.78
1	5	0	7340.71	0	5	1	5312.62	2	2	0	6338.91
1	3	1	7583.14	2	3	0	5497.74	0	0	4	6511.09
2	3	0	7583.35	1	3	1	5498.54	1	1	2	6550.25
0	3	2	7666.75	0	3	2	5541.23	1	3	1	6638.25
3	1	0	7775.94	3	1	0	5661.36	0	2	3	6685.24
2	1	1	7775.96	2	1	1	5661.56	1	5	0	6694.81
1	1	2	7933.60	1	1	2	5738.02	3	0	0	6799.72
0	1	3	7952.58	0	1	3	5755.18	0	4	2	6826.58
0	8	0	7996.69	0	8	0	5803.48	0	6	1	6932.35
0	6	1	8305.33	1	6	0	6019.91	0	8	0	6997.68
1	6	0	8309.45	0	6	1	6021.33	2	1	1	7159.94
1	4	1	8554.09	2	4	0	6208.42	2	3	0	7190.19
2	4	0	8554.71	1	4	1	6208.77	1	0	3	7291.76
0	4	2	8637.80	0	4	2	6251.19	0	1	4	7374.01
2	2	1	8746.36	3	2	0	6371.05	1	2	2	7406.32
3	2	0	8746.44	2	2	1	6371.14	1	4	1	7490.63
4	0	0	8894.03	1	2	2	6448.78	1	6	0	7541.14
3	0	1	8894.04	0	2	3	6463.05	0	3	3	7544.34
1	2	2	8906.73	0	9	0	6504.59	3	1	0	7644.41

approach (analogous to the force constants for H_2Se from the present work) are compared with ab initio values from Bartlett *et al.* (*28*) and values obtained by Halonen and Carrington (*4*) through fitting to experiment.

TABLE IV—*Continued*

$H_2{}^{80}Se$				$D_2{}^{80}Se$				$HD^{80}Se$			
v_1	v_2	v_3	/cm^{-1}	v_1	v_2	v_3	/cm^{-1}	v_1	v_2	v_3	/cm^{-1}
0	2	3	8920.27	4	0	0	6512.00	0	5	2	7680.07
0	9	0	8944.29	3	0	1	6512.03	0	7	1	7778.05
2	0	2	9139.75	2	0	2	6632.87	0	9	0	7833.50
1	0	3	9145.43	1	0	3	6639.84	2	0	2	7952.68
0	0	4	9232.45	0	0	4	6686.66	2	2	1	8007.46
0	7	1	9259.69	0	7	1	6724.65	0	0	5	8031.37
1	7	0	9266.32	1	7	0	6724.68	2	4	0	8034.60
1	5	1	9514.90	1	5	1	6914.24	1	1	3	8142.42
2	5	0	9515.76	2	5	0	6914.24	0	2	4	8230.60
0	5	2	9598.89	0	5	2	6956.50	1	3	2	8256.25
2	3	1	9708.55	3	3	0	7076.65	1	5	1	8335.48
3	3	0	9708.68	2	3	1	7076.66	1	7	0	8378.90
3	1	1	9852.53	1	3	2	7155.55	0	4	3	8396.39
4	1	0	9852.53	0	3	3	7166.91	3	2	0	8483.54
1	3	2	9871.72	0	10	0	7199.42	3	0	1	8487.43
0	3	3	9879.85	4	1	0	7215.67	0	6	2	8525.46
0	10	0	9880.95	3	1	1	7215.68	0	8	1	8614.58
				2	1	2	7337.93	0	10	0	8659.40
				1	1	3	7343.10	2	1	2	8795.25
				0	1	4	7388.85	1	0	4	8846.72
				0	8	1	7422.32	2	3	1	8848.75
				1	8	0	7423.76	2	5	0	8871.64
				1	6	1	7614.67	0	1	5	8891.43
				2	6	0	7614.92	4	0	0	8895.87
				0	6	2	7656.88	1	2	3	8987.71
				2	4	1	7777.82	0	3	4	9080.29
				3	4	0	7777.85	1	4	2	9099.67
				1	4	2	7858.00	1	6	1	9172.28
				0	4	3	7866.47	1	8	0	9207.62
				0	11	0	7887.73	0	5	3	9240.93
				3	2	1	7915.74	3	3	0	9316.55
				4	2	0	7915.75	3	1	1	9322.13
				5	0	0	8032.62	0	7	2	9362.26
				4	0	1	8032.62	0	9	1	9441.50
				2	2	2	8039.29	0	11	0	9475.59
				1	2	3	8042.83	0	0	6	9508.08
				0	2	4	8087.62	2	0	3	9555.01
				0	9	1	8114.08	2	2	2	9632.41
				1	9	0	8116.89	2	4	1	9683.19
				3	0	2	8199.38	1	1	4	9685.00
				2	0	3	8200.52	2	6	0	9700.90
				1	0	4	8274.00	4	1	0	9721.71
				0	0	5	8301.69	0	2	5	9742.04
				1	7	1	8309.78	1	3	3	9826.98
				2	7	0	8310.18	0	4	4	9922.11
				0	7	2	8352.04	1	5	2	9936.57

Comparison of Figs. 2 and 3 shows that in $D_2{}^{80}Se$, the cluster formation occurs at higher J values than are found for $H_2{}^{80}Se$. Semiclassical theory provides the expression

$$J_{CR} = \frac{\omega}{4A}\sqrt{\frac{A-B}{C}} \tag{13}$$

for the so-called critical J-value J_{CR} at which the deviation from the customary rigid rotor picture becomes apparent [see Eq. (4) of Ref. (*9*)]. In Eq. (13), ω is the normal

frequency of the bending mode and A, B, and C are the rotational constants. Using the rotational constants and the bending frequency from Ref. (*20*), we obtain $J_{CR} = 18$ for $D_2{}^{80}Se$. For $H_2{}^{80}Se$, the corresponding number is $J_{CR} = 12$ (*9*). Figures 2 and 3 show that the energy distance between the two rigid rotor doublets at highest energy starts decreasing at $J \approx 12$ for $H_2{}^{80}Se$ and at $J \approx 18$ for $D_2{}^{80}Se$, in good agreement with the semiclassical prediction.

The wavefunctions resulting from the MORBID calculation can be used to study the so-called localization of rotational states (*9, 11, 29*) found in H_2Se. In Ref. (*11*) we discussed this localization effect on the basis of the eigenfunctions of the Watson-type effective Hamiltonian used to analyze the experimental data. This discussion led to the introduction of the localized states (or wavefunctions) which we have briefly mentioned in Section II. The localized wavefunctions are illustrated by Fig. 2 of Ref. (*11*); as already mentioned they arise naturally in the semiclassical description of molecular rotation. In Ref. (*11*), the localized wavefunctions were obtained in terms of purely rotational eigenfunctions of a Watson-type effective Hamiltonian, whereas here we aim at obtaining the localized wavefunctions on the basis of the complete rotation–vibration eigenfunctions of the MORBID Hamiltonian.

Semiclassical theory predicts that of the four localized wavefunctions $|\psi_{\text{Localized}}; j\rangle$ ($j = 1, 2, 3, 4$) representing the four states in the cluster with highest energy in a given J multiplet, two will have angular momentum projections of $-\hbar J$ and $\hbar J$, respectively, along an axis A which approximately bisects the angle between the y- and z-axes in the molecule-fixed axis system used by MORBID [see Fig. 1 of Ref. (*1*)]. The two remaining functions will have angular momentum projections of $-\hbar J$ and $\hbar J$, respectively, along an axis A' which is obtained by subjecting A to a C_2 rotation (*30*) around the C_2 symmetry axis of the molecule in its equilibrium configuration.

The analysis of the MORBID wavefunctions (and the localized wavefunctions obtained from them) carried out in the present work can be summarized as follows:

(1) We express the MORBID eigenfunction of Eq. (6) in the "primitive" basis set $|n_1 n_3\rangle|v_2, |k|\rangle|J, k, M\rangle$, $-J \leq k \leq J$ (see Section II):

$$|i; \Gamma_{rv}\rangle = \sum_{n_1, n_3, v_2} \sum_{k=-J}^{J} c^{(i;\Gamma_{rv})}_{n_1, n_3, v_2, k} |n_1, n_3\rangle|v_2, |k|\rangle|J, k, M\rangle. \tag{14}$$

For this function, we define a k-probability as

$$p_k^{(i;\Gamma_{rv})} = \sum_{n_1, n_3, v_2} |c^{(i;\Gamma_{rv})}_{n_1, n_3, v_2, k}|^2. \tag{15}$$

Analogous k-probabilities have been used by Larsen and Brodersen (*31*) to discuss the labeling of cluster states in CF_4.

(2) We discuss here sets of four cluster states whose MORBID eigenfunctions we label as $|i; A_1\rangle$, $|i; A_2\rangle$, $|i; B_1\rangle$, and $|i; B_2\rangle$, respectively. Here, A_1, A_2, B_1, and B_2 are the four irreducible representations of the molecular symmetry group for H_2Se, $C_{2v}(M)$ (*30*); the four cluster states always span the reducible representation $A_1 + A_2 + B_1 + B_2$. If the four states $|i; A_1\rangle$, $|i; A_2\rangle$, $|i; B_1\rangle$, and $|i; B_2\rangle$ are exactly degenerate eigenfunctions for the molecular rotation–vibration Hamiltonian, we can consider them as an orthonormal basis set in the four-dimensional space of degenerate eigenfunctions. This choice of basis set is not unique since we can subject the four basis functions to an arbitrary unitary transformation (a rotation in the four-dimensional space of degenerate eigenfunctions) to obtain four new orthonormal basis functions

which are given as linear combinations of the functions $|i; A_1\rangle$, $|i; A_2\rangle$, $|i; B_1\rangle$, and $|i; B_2\rangle$. The localized wavefunctions $|\psi_{\text{Localized}}; j\rangle$ ($j = 1, 2, 3,$ or 4) represent one particular choice of this basis suggested by semiclassical theory. We can express the unitary transformation from symmetrized states $|i; A_1\rangle$, $|i; A_2\rangle$, $|i; B_1\rangle$, and $|i; B_2\rangle$ to localized states as

$$|\psi_{\text{Localized}}; j\rangle = c_{i;A_1}^{(j)} |i; A_1\rangle + c_{i;A_2}^{(j)} |i; A_2\rangle + c_{i;B_1}^{(j)} |i; B_1\rangle + c_{i;B_2}^{(j)} |i; B_2\rangle, \quad (16)$$

$j = 1, 2, 3,$ or 4. Obviously, if the functions $|i; A_1\rangle$, $|i; A_2\rangle$, $|i; B_1\rangle$, and $|i; B_2\rangle$ describe exactly degenerate states, the new functions $|\psi_{\text{Localized}}; j\rangle$ ($j = 1, 2, 3, 4$) are also degenerate eigenfunctions of the molecular rotation–vibration Hamiltonian [compare with Eq. (6) of Ref. (*11*)]. In reality the four cluster states will not be exactly degenerate, but the energy splittings between them will be so small that it is meaningful to carry out the transformation given by Eq. (16).

(3) The coefficients $c_{i;\Gamma_{\text{rv}}}^{(j)}$ of Eq. (16) are determined through the technique already described in Ref. (*11*). We use the fact that we can form symmetrized linear combinations of the localized wavefunctions $|\psi_{\text{Localized}}; j\rangle$ ($j = 1, 2, 3,$ or 4) as described, for example, in Ref. (*30*). In order to obtain the symmetrized functions we must know how the localized wavefunctions transform under the symmetry operations in the molecular symmetry group $C_{2v}(M)$. However, these transformation properties can be straightforwardly deduced from Fig. 2 of Ref. (*11*); the symmetry operations simply permute the four localized wavefunctions. The resulting symmetrized wavefunctions, which we can express as linear combinations of the localized wavefunctions, can be identified with the eigenstates of the MORBID Hamiltonian, and the linear (unitary) transformation from localized to symmetrized wavefunctions can be inverted to yield a unitary transformation expressing the localized functions as linear combinations of the MORBID eigenfunctions $|i; A_1\rangle$, $|i; A_2\rangle$, $|i; B_1\rangle$, and $|i; B_2\rangle$ [see Eq. (16)]. For example, the localized wavefunction $|\psi_{\text{Localized}}; 1\rangle$ is given by [see Eq. (7) of Ref. (*11*)]

$$|\psi_{\text{Localized}}; 1\rangle = 1/2(|i; A_1\rangle + |i; A_2\rangle + |i; B_1\rangle + |i; B_2\rangle), \quad (17)$$

corresponding to $c_{i;A_1}^{(j)} = c_{i;A_2}^{(j)} = c_{i;B_1}^{(j)} = c_{i;B_2}^{(j)} = 1/2$ in Eq. (16).

(4) The next step is to define a k-probability $p_k^{(j)}$ given for the function $|\psi_{\text{Localized}}; j\rangle$. We obtain

$$p_k^{(j)} = |c_{i;A_1}^{(j)}|^2 p_k^{(i;A_1)} + |c_{i;A_2}^{(j)}|^2 p_k^{(i;A_2)} + |c_{i;B_1}^{(j)}|^2 p_k^{(i;B_1)} + |c_{i;B_2}^{(j)}|^2 p_k^{(i;B_2)}, \quad (18)$$

where $p_k^{(i;\Gamma_{\text{rv}})}$ is given in Eq. (15).

(5) We intend to use the k-probabilities in Eq. (18) for identifying the two "localization" axes A and A' mentioned above. Toward this end, we rotate the localized wavefunctions around the molecule-fixed x-axis (the axis perpendicular to the molecular plane). We denote the function obtained by rotating $|\psi_{\text{Localized}}; j\rangle$ through an angle $-\varphi$ around the x-axis as $R_x^{(-\varphi)}|\psi_{\text{Localized}}; j\rangle$. We determine the angle φ such that the rotated function $R_x^{(-\varphi)}|\psi_{\text{Localized}}; j\rangle$ has the "sharpest" possible k distribution; i.e., by varying φ we aim at obtaining a rotated function $R_x^{(-\varphi)}|\psi_{\text{Localized}}; j\rangle$ which, for one particular k value, k_{Local}, say, has a k-probability $p_{k_{\text{Local}}} \approx 1$, and k-probabilities $p_k \approx 0$ for $k \neq k_{\text{Local}}$. This type of analysis was also used by Larsen and Brodersen (*31*) in defining cluster indices for CF_4.

Figure 4 presents k-probabilities calculated from Eq. (18) for localized states belonging to the cluster at the highest energy found in the vibrational ground state of

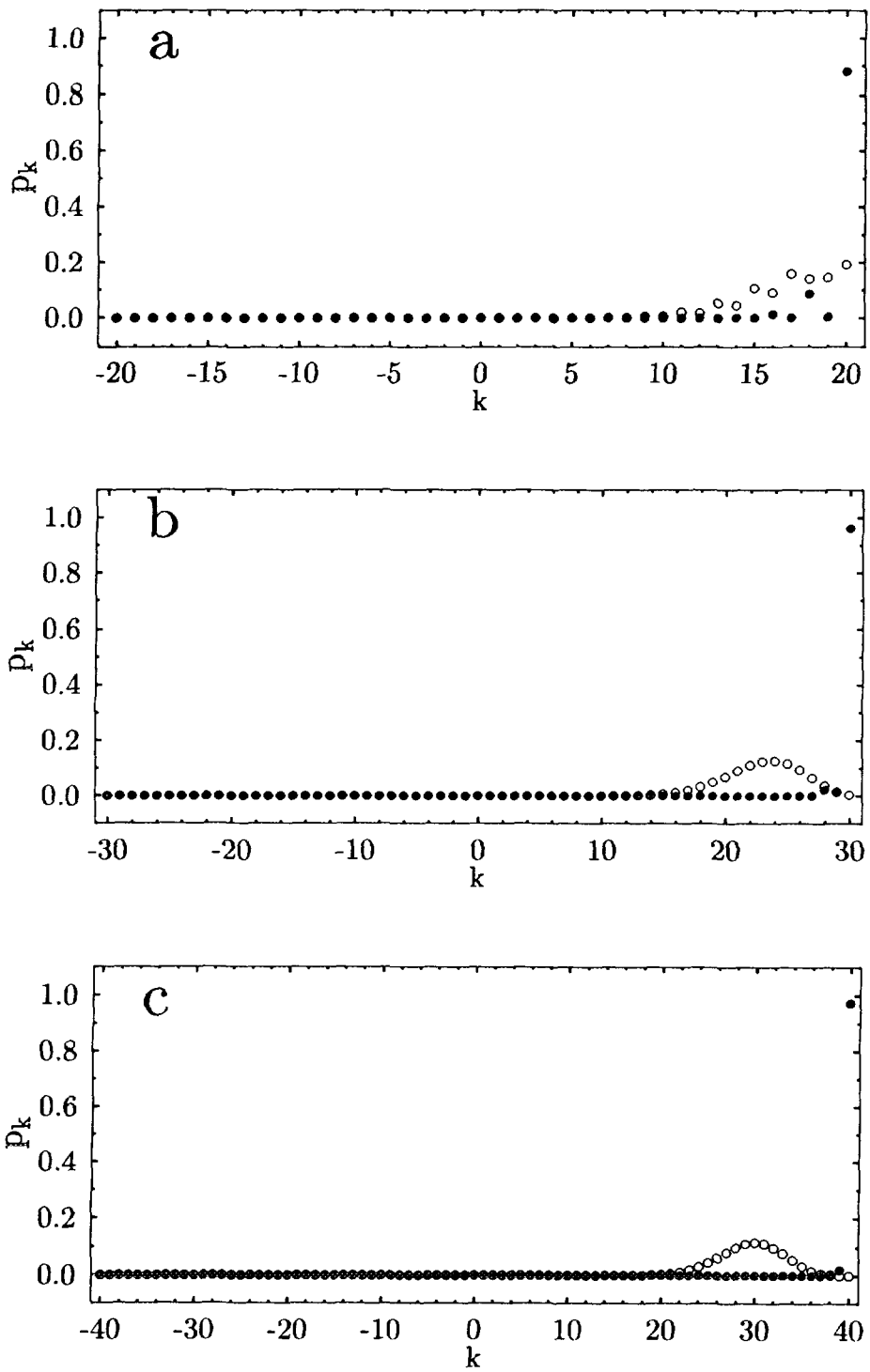

FIG. 4. The k-distributions of localized rotational states in the vibrational ground state of $H_2{}^{80}Se$. The figures show one state in the cluster at highest energy for (a) $J = 20$, (b) $J = 30$, and (c) $J = 40$, respectively. The empty circles show the k-probabilities p_k for the localized wavefunction $|\psi_{\text{Localized}}; 1\rangle$ [see Eq. (18)], and the filled circles show the analogous k-probabilities for the function $R_x^{(-\varphi)}|\psi_{\text{Localized}}; 1\rangle$ obtained by rotating $|\psi_{\text{Localized}}; 1\rangle$ through an angle $-\varphi$ around the molecule-fixed x-axis (the axis perpendicular to the molecular plane).

$H_2{}^{80}Se$ at $J = 20$, 30, and 40, respectively. The empty circles show the k-probabilities p_k for $|\psi_{\text{Localized}}; 1\rangle$; $k\hbar$ represents the projection of the total angular momentum on the molecule-fixed z-axis [see Fig. 1 of Ref. (*1*)]. The filled circles show k-probabilities for the rotated function $R_x^{(-\varphi)}|\psi_{\text{Localized}}; 1\rangle$. We have used $\varphi = 31°$ for $J = 20$, $\varphi = 40°$ for $J = 30$, and $\varphi = 42°$ for $J = 40$. These values of φ are in close agreement with the predictions from semiclassical theory (*11*). It is evident from Fig. 4 that when we rotate the wavefunction through the angle $-\varphi$ in the molecular plane, the dominant basis state in the resulting function has $k = J$. This means that the localized wavefunctions behave essentially as the eigenfunctions of a rigid symmetric top, but the defined projection of the total angular momentum is found along an axis that lies in the molecular plane and forms an angle φ with the molecule-fixed z-axis. Figure 4 shows that this localization becomes more pronounced as J increases (i.e., as the molecule approaches the classical limit), in agreement with the results obtained by Larsen and Brodersen (*31*) for CF_4. However, a closer inspection of the expansion coefficients $c^{(i;\Gamma_{rv})}_{n_1,n_3,v_2,K}$ of Eq. (6) shows that for increasing J, interactions between the basis functions representing the vibrational ground state and those representing excited vibrational states become increasingly important. For the cluster states at $J = 30$ shown in Fig. 4, about 80% of the contributions to the MORBID eigenfunctions originate in basis functions belonging to the vibrational ground state, while at $J = 40$ this contribution is only 50%. This is not surprising since in the variational MORBID scheme, centrifugal distortion effects are treated through interaction between vibrational basis states. Clearly these effects are important at $J = 40$ and must lead to considerable basis state mixing. One could say that as J increases, the localization of rotational states becomes stronger so that in a sense, the rotational motion becomes simpler. At the same time, however, the vibrational motion becomes more complicated due to the increasing interaction between basis states.

In the present work we have fitted energy level spacings involving $J \leqslant 5$. This part of the energy level spectrum is highly similar to that of a rigid asymmetric rotor with the equilibrium rotational constants of H_2Se. Nevertheless, MORBID provides a rather good prediction (Fig. 2) of the cluster structure as observed up to $J = 23$ which, as mentioned above, represents a significant qualitative deviation from the rigid rotor approximation. Hence MORBID has proved itself a useful tool for studying the cluster effects in H_2Se, and we intend to continue these studies through calculations of the rotational energy level structure in excited vibrational states.

ACKNOWLEDGMENTS

P.J. is very grateful to the Bergische Universität–Gesamthochschule Wuppertal, and in particular to R. J. Buenker, H. Bürger, and E. H. Fink, for a guest professorship in the period October 1992–July 1993. This work was supported by the Deutsche Forschungsgemeinschaft (through Grant Je 144/2-3) and by the Fonds der Chemischen Industrie. P.J. acknowledges further support from the Dr. Otto Röhm Gedächtnisstiftung and from the Fritz Thyssen-Stiftung. We are indebted to T. H. Edwards for sending us excerpts of Refs. (*22, 23*), and we thank R. H. Schwendeman for acting as an intermediary in this transaction. The present work has only been possible through the use of two supercomputers recently made available to us by the State of Hessen: the Siemens/Nixdorf S400/40 installation at the Technical University Darmstadt and the Siemens/Nixdorf S100/10 installation at the Justus Liebig University Giessen. The major part of the calculations reported here were carried out on these installations, and we are grateful for generous allotments of computer time. We thank N. Conrad of the Giessen computer center for particular help. Initial calculations were carried out on the CDC Cyber 960 installation at the Giessen computer center and on the Cray Y-MP2/232 installation of the Deutsche Forschungs- und Versuchsanstalt für Luft- und Raumfahrt (DLR), Oberpfaffenhofen near Munich. We are very grateful to the DLR, and particularly to D. Hausamann, for computer time granted within the collaboration scheme between the DLR and the Justus Liebig University

Giessen. We thank P. R. Bunker, B. P. Winnewisser, and M. Winnewisser for critically reading the manuscript and suggesting improvements, and S. Brodersen for communicating his results prior to publication.

RECEIVED: February 17, 1993

REFERENCES

1. P. JENSEN, *J. Mol. Spectrosc.* **128,** 478–501 (1988).
2. P. JENSEN, *J. Chem. Soc. Faraday Trans. 2* **84,** 1315–1340 (1988).
3. I. M. MILLS AND A. G. ROBIETTE, *Mol. Phys.* **56,** 743–765 (1985).
4. L. HALONEN AND T. CARRINGTON, JR., *J. Chem. Phys.* **88,** 4171–4185 (1988).
5. B. I. ZHILINSKII AND I. M. PAVLICHENKOV, *Opt. Spectrosc. (USSR)* **64,** 688–690 (1988). [In Russian]
6. J. MAKAREWICZ AND J. PYKA, *Mol. Phys.* **68,** 107–127 (1989).
7. J. MAKAREWICZ, *Mol. Phys.* **69,** 903–921 (1990).
8. J. PYKA, *Mol. Phys.* **70,** 547–561 (1990).
9. I. N. KOZIN, S. P. BELOV, O. L. POLYANSKY, AND M. YU. TRETYAKOV, *J. Mol. Spectrosc.* **152,** 13–28 (1992).
10. I. N. KOZIN, O. L. POLYANSKY, S. I. PRIPOLZIN, AND V. L. VAKS, *J. Mol. Spectrosc.* **156,** 504–506 (1992).
11. I. N. KOZIN, S. KLEE, P. JENSEN, O. L. POLYANSKY, AND I. M. PAVLICHENKOV, *J. Mol. Spectrosc.*, **158,** 409–422 (1993).
12. S. CARTER AND N. C. HANDY, *Comp. Phys. Rep.* **5,** 115–171 (1986).
13. J. TENNYSON, *Comp. Phys. Rep.* **4,** 1–36 (1986).
14. Z. BAČIĆ AND J. C. LIGHT, *Annu. Rev. Phys. Chem.* **40,** 469–489 (1989).
15. J. SENEKOWITSCH, A. ZILCH, S. CARTER, H.-J. WERNER, P. ROSMUS, AND P. BOTSCHWINA, *Chem. Phys.* **122,** 375–386 (1988).
16. J. A. FERNLEY, S. MILLER, AND J. TENNYSON, *J. Mol. Spectrosc.* **150,** 597–609 (1991).
17. E. KAUPPI AND L. HALONEN, *J. Phys. Chem.* **94,** 5779–5785 (1990).
18. P. JENSEN, *J. Mol. Spectrosc.* **133,** 438–460 (1989).
19. P. JENSEN, *Comp. Phys. Rep.* **1,** 1–55 (1983).
20. E. D. PALIK, *J. Mol. Spectrosc.* **3,** 259–295 (1959).
21. R. A. HILL AND T. H. EDWARDS, *J. Chem. Phys.* **42,** 1391–1396 (1965).
22. J. R. GILLIS, Ph.D. Dissertation, Michigan State University, 1979.
23. W. C. LANE, Ph.D. Dissertation, Michigan State University, 1984.
24. J. R. GILLIS AND T. H. EDWARDS, *J. Mol. Spectrosc.* **81,** 373–389 (1980).
25. J. R. GILLIS AND T. H. EDWARDS, *J. Mol. Spectrosc.* **85,** 74–84 (1981).
26. W. C. LANE, T. H. EDWARDS, J. R. GILLIS, F. S. BONOMO, AND F. J. MURCRAY, *J. Mol. Spectrosc.* **107,** 306–317 (1984).
27. P. HELMINGER AND F. C. DE LUCIA, *J. Mol. Spectrosc.* **58,** 375–383 (1975).
28. R. J. BARTLETT, S. J. COLE, G. D. PURVIS, W. C. ERMLER, H. C. HSIEH, AND I. SHAVITT, *J. Chem. Phys.* **87,** 6579–6591 (1987).
29. I. M. PAVLICHENKOV AND B. I. ZHILINSKII, *Ann. Phys. (NY)* **184,** 1–32 (1988).
30. P. R. BUNKER, "Molecular Symmetry and Spectroscopy," Academic Press, London, 1979.
31. S. G. LARSEN AND S. BRODERSEN, *J. Mol. Spectrosc.* **157,** 220–236 (1993).